Carrier Phase Distortions with anti-jamming Techniques using GNSS Array Receivers

Tobias Bamberg*†, Michael Meurer *†
* *Institute of Communications and Navigation, German Aerospace Center (DLR), Oberpfaffenhofen, Germany*
† *Chair of Navigation, RWTH Aachen University, Germany*
Email: tobias.bamberg@dlr.de

***Abstract*—The use of GNSS positioning in highly automated systems, like packet delivering using drones or self-driving cars, demands a reliable and accurate position estimation. At the same time the risk for radio frequency interference (RFI), intentional or unintentional, increases. A promising countermeasure to this issue is RFI mitigation with spatial filters using an antenna array. However, these filters can induces a phase error to the carrier phase measurements used with high precision positioning techniques like Precise Point Positioning (PPP). In this work the induced carrier phase error is studied for some common spatial filters like the minimum variance distortionless response (MVDR) or the Eigenbeamformer.**

***Index Terms*—GNSS, carrier phase measurement, antenna array, beamforming, spatial filter, RTK, PPP**

I. Introduction

Global navigation satellite systems (GNSS) are widely used for positioning and timing. The systems are used by almost every land, air and water vessel to help navigate or to navigate. The increasing number of private and commercial UAVs and the upcoming of autonomous driving cars will even increase the number of systems relying on GNSS. Therefore it is getting more and more important to secure the availability of the position, velocity and time (PVT) solution even in the presence of jamming or spoofing signals. Furthermore the new applications demand a higher precision of the PVT solution. The latter demand can be fulfilled by the Precise Point Positioning (PPP) and Real Time Kinematics (RTK) techniques. One key element of these approaches is the utilization of carrier phase measurements while computing PVT solution. The carrier phase measurements allow to deliver much more accurate range measurements since the wavelength of a GNSS carrier, e.g. 19 centimeter for GPS L1, is much smaller than a PRN code chip, e.g. 293 meter with C/A code of GPS L1.

An advanced approach for protection against jamming and spoofing is provided by using adaptive antenna arrays and utilizing signal processing in the spatial domain. The antenna arrays can be used for detection and mitigation of jammers[1] and spoofers[2]. The mitigation is usually conducted by spatial filters like the minimum variance distortionless response (MVDR) filter[3]. However, these filters induce a carrier phase error into the measurements degrading the precision of PPP and RTK solutions or making it even impossible to calculate those. For an ideal antenna array, the MVDR filter is theoretically free of distortions[4], but it needs to know the steering vector of the incoming satellite signal. The steering vector of an impinging signal is its spatial signature containing the gain and phase information of the signal at each antenna element. With real antenna arrays the corresponding steering vectors have to be obtained in a calibration process that is accompanied by measurement errors due to different processing components, temperatures, cable length etc. Therefore in practice, even MVDR induces some phase distortions.

Jia et al [4] investigate the effect of the MVDR and power inversion (PI) filters on the carrier measurement and compares them to a compensation approach that aims to preserve the continuity of the phase measurement in jammed scenarios. However, [4] does only analyze short time simulations with a jamming incident of 20 milliseconds. Simulations have shown that the long term stability is not necessarily given. Daneshmand et al [5] proposes a modified PI filter that is able to compensate the phase bias even for uncalibrated antenna arrays but at the cost of half of the degrees of freedom in radio frequency interference (RFI) suppression and also only for a centro-symmetrical array geometry.

To extend the ongoing research and to pave the way for using PPP and RTK with adaptive antenna arrays, this work is going to analyze the amount of distortion the different spatial filters induce in different scenarios in a systematic way with and without RFI. Therefore three different blind and one deterministic beamforming approaches are compared. Blind means here without any knowledge about the antenna gain/phase matrix, calibration matrix and the direction of arrival of the RFI. The four beamformers will be compared in a scenario with three different jammers. This paper extends the research conducted in [6].

II. System Model and Spatial Signal Processing

In this section the signal model and the theoretical background for the spatial filters and beamformer will be introduced. In the last part of this section the error of the spatial signal

processing on the carrier phase measurement will be analyzed on a theoretical basis.

A. Signal Model

The following formula describes the impinging signal on an antenna array with N antennas for M satellites and L jamming signals:

$$\mathbb{C}^{N\times 1} \ni \mathbf{x}(t) = \sum_{m=1}^{M} \mathbf{a}_m s_m(t) + \sum_{l=1}^{L} \mathbf{a}_l j_l(t) + \mathbf{n} \quad (1)$$

$$= \mathbf{s} \qquad + \mathbf{j} \qquad + \mathbf{n} \quad (2)$$

$\mathbf{a}_m \in \mathbb{C}^{N\times 1}$ and $\mathbf{a}_l \in \mathbb{C}^{N\times 1}$ describe the steering vectors for the satellite and the jamming signal, respectively. The steering vector depends on the direction of arrival (DoA) of the impinging signal and the antenna array. For an ideal antenna array $\mathbf{a} = \left(e^{-\mathrm{j}\,\mathbf{k}^{\mathrm{T}}\mathbf{r}_1}, \ldots, e^{-\mathrm{j}\,\mathbf{k}^{\mathrm{T}}\mathbf{r}_N}\right)^{\mathrm{T}}$ describes the steering vector for an impinging wave with the wave vector $\mathbf{k}$ and the spatial positions $\mathbf{r}_1, \ldots, \mathbf{r}_N$ of the antenna elements. At this point it shall be emphasized that the steering vector also depends on the choice of the reference coordinate system. The point of origin of this reference system is the spatial and phase reference for the modeled signal $s_m(t)$ and $j(t)$. In this paper this point of origin is always the center of the antenna array determined as the mean of all antenna positions.
$s_m(t)$ describes the satellite signal. It contains the data bits, the spreading code, and the carrier signal. j_l stands for the jamming signal and $\mathbf{n} \in \mathbb{C}^{N\times 1}$ stands for the additive noise term. It is modeled as temporally and spatially white Gaussian Noise with zero mean and a variance of $\sigma^2_{\mathbf{n}}$.

B. Spatial Filter and Beamformer

Combining the received antenna signals enables the possibility to amplify or to suppress different DoAs. Therefore the received signals are multiplied with a complex number and summed up. The beamformed signal can be expressed as

$$y = \mathbf{w}^{\mathrm{H}}\mathbf{x}. \quad (3)$$

The weight vector $\mathbf{w}$ is computed by the used spatial filter. A common way to suppress unwanted signals is to use the minimum variance (MV) filter, which minimizes the variance of the unwanted signals in the output signal. Assuming that the unwanted signals have zero mean and are uncorrelated with the satellite signal, we can write:

$$\min_{\mathbf{w}} \mathrm{var}\left[\mathbf{w}^{\mathrm{H}}\left(\mathbf{j}+\mathbf{n}\right)\right] = \mathbf{w}^{\mathrm{H}}\mathbf{R}_{\mathbf{j}+\mathbf{n}}\mathbf{w} \quad (4)$$

$\mathbf{R}_{\mathbf{j}+\mathbf{n}}$ is the covariance matrix of the unwanted signal plus the noise. To exclude the trivial solution $\mathbf{w} = \mathbf{0}$, another condition needs to be added. The additional condition $\mathbf{w}^{\mathrm{H}}\mathbf{a}_m = 1$ yields the MVDR filter. The solution for this filter is given by:

$$\mathbf{w}_{\mathrm{MVDR}} = \frac{\mathbf{R}^{-1}_{\mathbf{j}+\mathbf{n}}\mathbf{a}_m}{{\mathbf{a}_m}^{\mathrm{H}}\mathbf{R}^{-1}_{\mathbf{j}+\mathbf{n}}\mathbf{a}_m} \quad (5)$$

The impinging satellites signals are far below the noise floor. Therefore, in practice the covariance matrix of the unwanted signal can be approximated without any prior knowledge by:

$$\widetilde{\mathbf{R}} = \frac{1}{K}\sum_{k=1}^{K}\mathbf{x}[k]\mathbf{x}[k]^{\mathrm{H}}, \quad (6)$$

where K describes the number of used samples and $\mathbf{x}[k]$ represent the read samples at the time instance $t_k = kT$. T is the sampling interval.
The calculation of the steering vector for the desired satellite signal is more delicate. There are different ways to overcome this issue:
If the reception pattern of the receiver system, the attitude and the position of the antenna array are known, the DoA and the steering vector of the impinging signal can be calculated using the ephemeris data. This approach is classified as a deterministic filter. In practice this approach is quite challenging due to the temporal change of the needed information. One promising attempt to estimate the time changing components jointly is described by Zorn in [7] and [8].
Another way is quite common in the literature: Instead of an individual steering vector for every satellite, a common spatial filter with a constant beamformer is applied for all satellites. The formula for the weight vector changes then to:

$$\mathbf{w}_{\mathrm{MVConst}} = \frac{\mathbf{R}^{-1}_{\mathbf{j}+\mathbf{n}}\mathbf{k}}{\mathbf{k}^{\mathrm{H}}\mathbf{R}^{-1}_{\mathbf{j}+\mathbf{n}}\mathbf{k}} \quad (7)$$

$\mathbf{k} \in \mathbb{C}^{N\times 1}$ is an arbituary vector but not zero (e.g. $(1, 0, \ldots, 0)^{\mathrm{T}}$). In the literature it is quite common to call this approach power inversion filter[4][9]. This approach has the advantage that no additional information about the antenna characteristics are required and is therefore classified as a blind approach. However, this approach only suppresses unwanted signals, but does not amplify the specific satellite signals. It will suppress satellite signals as well, if the DoA is similar to the one of the unwanted signal.

C. Eigenbeamformer

Another way to calculate the steering vector is to estimate it after the de-spreading/correlation. The correlation amplifies the wanted signal over the noise floor making it possible to extract its spatial signature.
With this approach it is common to apply prewhitening prior to PRN-code correlation so that the resulting signal reads:

$$\bar{\mathbf{x}}(t) = \mathbf{R}^{-1}_{\mathbf{j}+\mathbf{n}}\mathbf{x}(t) \quad (8)$$

Then the signal after correlation can be expressed as:

$$\mathbf{y}_m = G_m\mathbf{R}^{-1}_{\mathbf{j}+\mathbf{n}}\mathbf{a}_m + \mathbf{n}_{\mathrm{pc},m} \quad (9)$$

with the factor G_m representing the scaling of the correlation with the local replica and $\mathbf{n}_{\mathrm{pc},m}$ is the noise after the correlation

process. This noise contains the other satellites as well as the suppressed jammers and the pre-correlation noise.
Calculating the Eigenvalue decomposition and taking the Eigenvector, which belongs to the strongest Eigenvalue yields the filtered steering vector: $\bar{\tilde{\mathbf{a}}}_m$. Due to this step, the beamformer is called Eigenbeamformer.
This approach does not need any information about the antenna array and is therefore also classified as a blind filter. The Eigenbeamformer is described in [10] and [4] in more detail.
The weighting vector for the constrained MV filter with a Eigenbeamformer is given by:

$$\mathbf{w}_{\text{MVEig}} = \frac{\mathbf{R}_{\mathbf{j}+\mathbf{n}}^{-1}\bar{\tilde{\mathbf{a}}}_m}{\bar{\tilde{\mathbf{a}}}_m{}^{\text{H}}\mathbf{R}_{\mathbf{j}+\mathbf{n}}^{-1}\bar{\tilde{\mathbf{a}}}_m} \tag{10}$$

D. Problem Statement

Using the previously mentioned spatial filters and beamformer will suppress unwanted signals and – in some case – amplify the wanted signals. It is basically reached by summing up phase shifted signals. The resulting sum signal is then forwarded to the PLL/DLL, which are used to get the pseudorange and carrier phase measurements. Therefore the spatial filters and beamformer will affect the carrier phase measurements. Mathematically the effect can be seen in combining equation (3) and (1):

$$y = \mathbf{w}^{\text{H}}\mathbf{x} = \sum_{m=1}^{M}\mathbf{w}^{\text{H}}\mathbf{a}_m s_m(t) + \sum_{l=1}^{L}\mathbf{w}^{\text{H}}\mathbf{a}_l j_l + \mathbf{w}^{\text{H}}\mathbf{n}. \tag{11}$$

The induced phase shift on a single satellite signal s_m due to spatial signal processing can be described as the phase of the product of the weighting vector and the true steering vector of this particular satellite:

$$\Delta\varphi_m = \angle\mathbf{w}^{\text{H}}\mathbf{a}_m. \tag{12}$$

It is trivial to show that, ideally, the MVDR does not induce any phase error due to its additional condition: $\mathbf{w}^{\text{H}}\hat{\mathbf{a}}_m = 1$. This is true even if the covariance matrix is erroneous and the suppression of the unwanted signals is reduced. However, in practical applications the steering vector $\hat{\mathbf{a}}_m$ is not known exactly (i.e. $\hat{\mathbf{a}}_m \neq \mathbf{a}_m$) due to imperfect knowledge of the DoA and the reception pattern of the system. Therefore in practice even the MVDR induces some phase error.

III. Simulations

A. Simulation Environment

The simulation environment was implemented using the software MATLAB. The simulated signals are generated in baseband while accounting for the Doppler effect. The output of the antenna array system is obtained by multiplying the satellite signals with the corresponding steering vector. Afterwards every channel is superposed with Gaussian noise.
Figure 1 shows the functional diagram of the receiver. The N input signals are spatially filtered using the inverse of the covariance matrix (prewhitening). After the despreading/correlation, the incoming signal is beamformed individually for each satellite. The prewhitening and the beamforming can be described together with a single weighting vector $\mathbf{w}$. The separation of these in the implementation is due to the Eigenbeamformer, which needs the spatial information after the correlation. The PLL and DLL operate only on a single signal. Therefore they are implemented like in a common single antenna receiver. The described steps are evaluated separately for each satellite 1 to M.

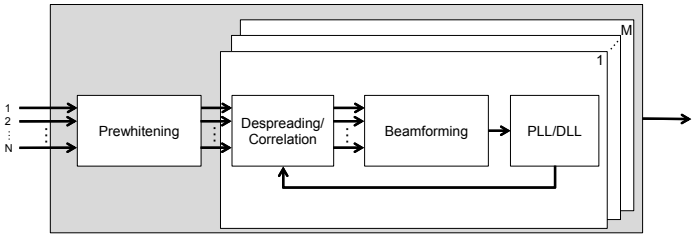

Fig. 1: Implemented receiver structure with N Antennas.

B. Implemented Spatial Filter and Beamformer

During the simulations the following spatial filter/beamformer were analyzed:

1) **MVDR**. Estimated covariance matrix and true steering vector. In Formula:

$$\mathbf{w}_{\text{MVDR}} = \frac{\widetilde{\mathbf{R}}^{-1}\mathbf{a}_m}{\mathbf{a}_m{}^{\text{H}}\widetilde{\mathbf{R}}^{-1}\mathbf{a}_m} \tag{13}$$

2) **MVConst**: Prewhitening and Constant Beamformer. This filter is further separated into two approaches:
   a) $\text{MVConst}_{\mathbf{e}_1}$ uses the standard unit vector $\mathbf{e}_1$ as the constant beamformer:

$$\mathbf{w}_{\text{MVConst}_{\mathbf{e}_1}} = \frac{\widetilde{\mathbf{R}}^{-1}\mathbf{e}_1}{\mathbf{e}_1{}^{\text{H}}\widetilde{\mathbf{R}}^{-1}\mathbf{e}_1} \tag{14}$$

   b) $\text{MVConst}_{\mathbf{1}}$ uses a column vector containing N "ones":

$$\mathbf{w}_{\text{MVConst}_{\mathbf{1}}} = \frac{\widetilde{\mathbf{R}}^{-1}\mathbf{1}_{N\times 1}}{\mathbf{1}_{N\times 1}{}^{\text{H}}\widetilde{\mathbf{R}}^{-1}\mathbf{1}_{N\times 1}} \tag{15}$$

3) **MVEig**: Prewhitening and Eigenbeamformer. This filter applies the spatial filter and Eigenbeamformer as it is described in the previous section:

$$\mathbf{w}_{\text{MVEig}} = \frac{\widetilde{\mathbf{R}}^{-1}\bar{\tilde{\mathbf{a}}}_m}{\bar{\tilde{\mathbf{a}}}_m{}^{\text{H}}\widetilde{\mathbf{R}}^{-1}\bar{\tilde{\mathbf{a}}}_m} \tag{16}$$

Except for the MVDR filter all these approaches can be used without any additional knowledge about the antenna array.

TABLE I: Jammer settings used in the simulations.

Jammer	Azimuth	Elevation	S/N	J/S	On	Off
J_1	308°	5°	30 dB	48 dB	250 ms	500 ms
J_2	72°	35°	30 dB	48 dB	500 ms	750 ms
J_3	250°	65°	30 dB	48 dB	750 ms	1000 ms

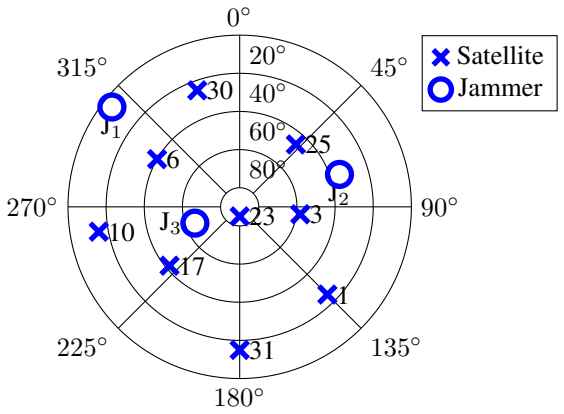

Fig. 2: Constellation used for the simulations. "x" marks the DoA of a satellite and "o" marks the DoA of a jammer.

C. Scenario

The scenario was chosen to analyze the induced phase error of the introduced beamformer in different jamming situations. The position of the satellites and the user position in the simulation are static, but during the simulation run three different jammers are switched on/off. The simulated time is one second with a sampling rate of 2.1 megahertz. The covariance matrices and the beamformers are updated every millisecond. Due to the limited number of samples after the correlation, the calculation of the post-correlation covariance matrix is conducted using a sliding window of 20 post-correlation samples.

The simulation is divided into four parts of a duration of 250 milliseconds: The first part (0 to 250 milliseconds) is free of any RFI. In the second part (250 to 500 milliseconds) jammer J_1 is active. In the third part jammer J_2 and in the fourth part jammer J_3 is active. The intervals of the jammer do not overlap. Table I shows the settings of the jammer and Fig. 2 visualizes the used constellation including the three jammers.

The signal generator uses the measured reception pattern of the DLR GALANT antenna array [11] to generate the incoming signals. For the analysis of the MVDR, the simulated receiver assumes a simplified antenna array model (the steering vector only depends on the geometric distances). The DoA of the satellite signals are assumed to be known.

To calculate the induced phase error, the phase of the product of the applied beamformer and the steering vector was evaluated ($\angle \mathbf{w}^{\mathrm{H}} \mathbf{a}_m$). The steering vector in this product is always the one, which has been used for the signal generation.

D. Simulation Results

In this section the simulations results will be shown and commented. Figure 3 shows the induced phase error for one simulation run for the different beamformers over the simulation time of one second. The Tables II show the mean and standard deviation for 500 Monte Carlo simulations of this scenario. The results are separated into the different beamformers. As described in the scenario description, the MVDR assumes a simplified antenna array model even though the signal generator uses a measured pattern. Beamformer $\mathrm{MVConst}_{\mathbf{e}_1}$ and MVEig induce a deterministic phase bias, because they are referred to the first antenna element [6] instead of the center of the antenna array. This deterministic phase bias has been calculated using the geometry of the array and subtracted to make all four approaches comparable.

Without any RFI, the mean values of the phase errors are small. $\mathrm{MVConst}_{\mathbf{e}_1}$ and MVEig show the same tendency. The mean is not zero due to the discrepancy of the measured antenna pattern and the simplified antenna array pattern. MVDR also suffers from this discrepancy (otherwise it would have no phase error at all as mentioned in II-D). However, due to the low sensitivity of the MVDR filter [6] the effect is less several. $\mathrm{MVConst}_{\mathbf{1}}$ shows a low mean error for PRN23, which is almost in the zenith, but shows higher error for lower satellites. This has been expected, because the constant beamformer used in this case represents the steering vector of a satellite in the zenith for a simplified antenna array.

Adding a jammer to the scenario results in a change of the mean phase error. The beamformers $\mathrm{MVConst}_{\mathbf{e}_1}$ and MVEig have a similar mean phase error and the highest change. The standard deviation is higher for MVEig, especially for satellites that are close to the suppressed area (PRN06, PRN30 for J_1. PRN25 for J_2. PRN10, PRN17 for J_3). The reason is that MVEig estimates the steering vector after the correlation, which becomes more challenging for a suppressed satellite signal. MVDR is affected least for all three different jammers. The highest mean values by magnitude are those that are close to a suppressed area. In the case of $\mathrm{MVConst}_{\mathbf{1}}$, the mean error highly depends on the situation. Ignoring PRN10 shows that the mean phase error for this beamformer is low in the presence of J_1 and J_2. This matches with the results found in [6]. However, for a jammer with a higher elevation (J_3) the beamformer tend to induce a phase shift of almost 180 degrees to some satellites (PRN10, PRN17, PRN31). These satellites are all in the same part of the hemisphere like the jammer. This effect can be visualized by plotting the phase error of the beamformer over the upper hemisphere (Fig. 4). The beamformer induces a phase shift of about 180 degrees to all satellites that have a lower elevation than the jammer and are located in the same direction as the jammer.

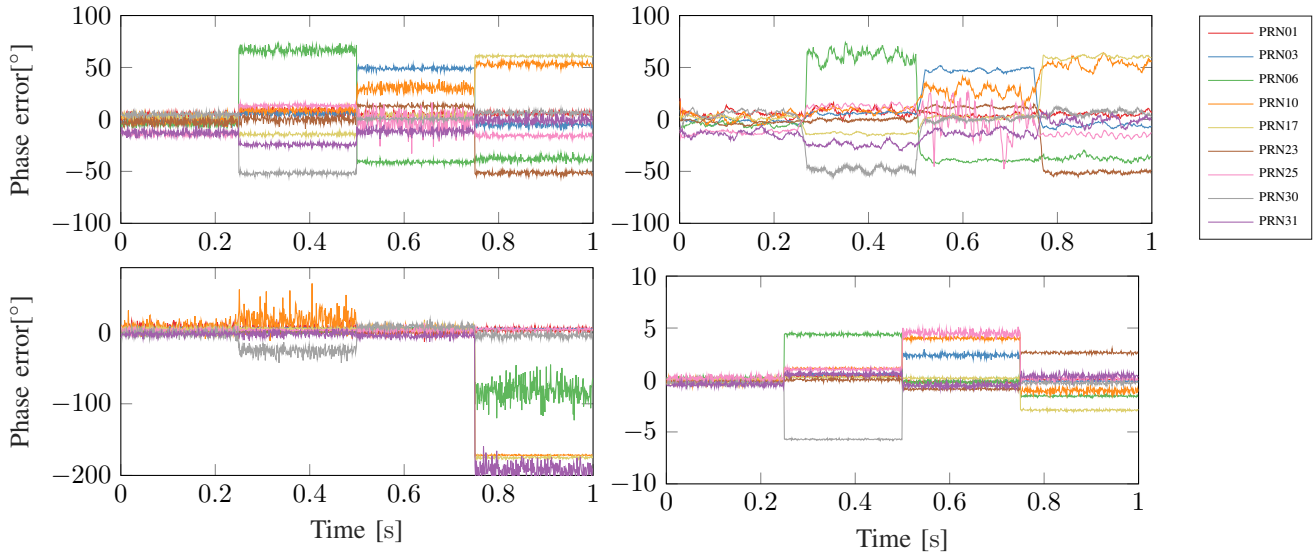

Fig. 3: Phase error induced by the spatial processing of the four spatial filter/beamformer: $\text{MVConst}_{\mathbf{e}_1}$ (top left), MVEig (top right), $\text{MVConst}_{\mathbf{1}}$ (bottom left) and MVDR (bottom right). The scale of the y-axis of the bottom plot differs from the rest to show the complete plot.

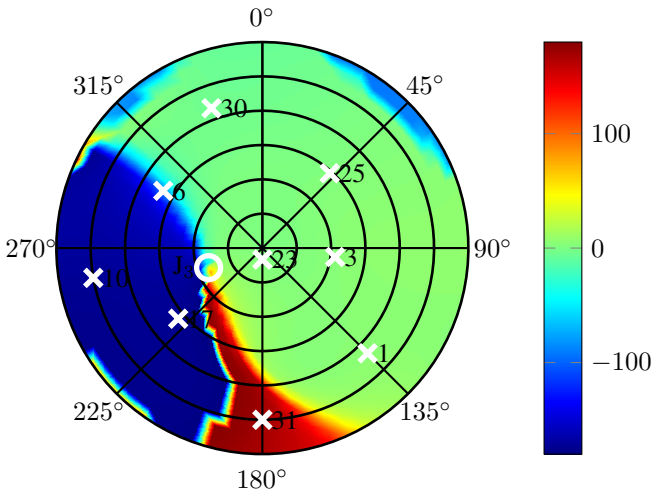

Fig. 4: Phase error in degree [°] of beamformer $\text{MVConst}_{\mathbf{1}}$ over upper hemisphere in the last part of the simulation (J_3 is active).

IV. Conclusion

The simulations have mostly confirmed the results of [6]: The MVDR filter is quite forgiving regarding small errors of the assumed steering vector. So in general, if the DoA of the signals and the antenna array pattern are approximately known, it is recommendable to use those information by applying an MVDR filter. The resulting phase variation and offset is reasonable small and therefore this filter will most likely work together with a carrier phase measurement based algorithm like PPP/RTK.

The MVEig beamformer is an option, if the steering vector for the incoming signal is unknown, but it is wanted to amplify the individual incoming signals. However, this beamformer induces different phase errors for different jammer. In a changing environment the phase error will be varying making it difficult for PPP/RTK to work properly. Without an additional method to keep the phase offset continuous these algorithms can hardly be used. Further research is necessary at this point.

The beamformer $\text{MVConst}_{\mathbf{e}_1}$ induces a similar phase error and without additional research it can hardly be used with PPP/RTK. This beamformer does not amplify individual signal, therefore it does not apply one advantage of an antenna array. On the other hand, for this beamformer the computational effort does not increase with the number of satellites, because it calculates only one beamformer for all satellites.

For a planar and simplified antenna array, $\text{MVConst}_{\mathbf{1}}$ amplifies signals coming from the zenith and makes sure that these signals are not affected by any phase error. However, in the same array it will completely suppress signals that are coming from an elevation of 0 degree and an azimuth of 0, 90, 180 or 270 degrees. The simulations have shown that the phase error for this beamformer is small for most of the satellites, especially if the jammer has a low elevation. However, large phase error can be observed in the case of a high elevation of the jammer. Plotting the phase error over the whole upper hemisphere showed that the phase error is most-likely around 0 or 180 degrees. It could be an option to account for this behavior in the carrier-phase tracking algorithms. Summing up, $\text{MVConst}_{\mathbf{1}}$ can most likely

TABLE II: Phase error in degree [°] induced by the spatial processing of the four different spatial filter/beamformer. The results are separately for each jammer.

	No Jammer							
	$\text{MVConst}_{\mathbf{e}_1}$		MVEig		MVDR		$\text{MVConst}_{\mathbf{1}}$	
	Mean	Std	Mean	Std	Mean	Std	Mean	Std
PRN01	4.08	2.13	3.73	2.64	-0.05	0.07	4.97	4.39
PRN03	-1.93	1.84	-1.63	1.97	0.12	0.04	5.65	0.58
PRN06	-4.35	1.79	-3.94	1.84	0.17	0.10	2.56	2.31
PRN10	0.42	2.98	0.41	3.46	-0.12	0.17	6.77	6.64
PRN17	2.43	1.62	1.95	1.65	0.07	0.06	4.67	2.27
PRN23	-2.64	2.66	-3.00	1.36	-0.13	0.07	-0.02	0.09
PRN25	-13.69	1.75	-12.88	1.74	0.18	0.18	1.98	2.46
PRN30	4.77	1.88	4.58	3.16	-0.33	0.11	-2.51	4.23
PRN31	-13.01	2.35	-13.29	3.04	-0.42	0.16	-2.58	2.20
RMS	6.93	2.16	6.74	2.43	0.21	0.12	4.05	3.38
Std	6.40	0.44	6.18	0.72	0.20	0.05	3.27	1.90

	Jammer 1							
	$\text{MVConst}_{\mathbf{e}_1}$		MVEig		MVDR		$\text{MVConst}_{\mathbf{1}}$	
	Mean	Std	Mean	Std	Mean	Std	Mean	Std
PRN01	8.08	2.22	7.05	3.51	0.40	0.08	6.53	3.89
PRN03	5.81	1.30	5.63	1.36	0.53	0.06	5.76	0.88
PRN06	66.84	2.86	57.43	6.60	4.39	0.10	-0.78	1.17
PRN10	8.96	1.67	8.89	2.40	1.10	0.06	68.15	126.04
PRN17	-14.32	1.16	-13.73	1.25	0.26	0.05	4.88	1.07
PRN23	-0.05	2.37	-0.69	1.36	0.02	0.09	0.27	0.15
PRN25	13.17	1.17	12.61	1.96	1.02	0.09	2.66	0.76
PRN30	-51.87	1.16	-48.22	3.25	-5.71	0.04	-26.22	5.23
PRN31	-24.27	1.20	-24.04	2.22	0.57	0.13	-2.33	2.86
RMS	30.38	1.79	27.30	3.10	2.47	0.08	24.60	42.09
Std	30.35	0.61	27.30	1.59	2.46	0.03	23.71	39.01

	Jammer 2							
	$\text{MVConst}_{\mathbf{e}_1}$		MVEig		MVDR		$\text{MVConst}_{\mathbf{1}}$	
	Mean	Std	Mean	Std	Mean	Std	Mean	Std
PRN01	4.21	1.73	4.18	2.48	-0.19	0.06	0.54	3.75
PRN03	48.91	1.30	47.68	1.62	2.37	0.14	5.65	1.48
PRN06	-41.20	1.11	-39.79	1.61	-0.18	0.14	5.28	0.51
PRN10	30.01	3.10	27.98	6.21	4.01	0.11	4.21	3.27
PRN17	3.71	1.70	3.23	1.56	0.17	0.06	4.99	2.31
PRN23	12.71	1.29	12.35	1.00	-0.87	0.07	-0.99	0.12
PRN25	-0.63	7.60	-2.34	13.29	4.51	0.23	2.88	2.61
PRN30	0.71	1.17	1.04	1.92	-0.56	0.04	7.18	2.77
PRN31	-11.12	2.22	-11.71	3.11	-0.54	0.16	-4.92	2.43
RMS	24.29	3.06	23.48	5.20	2.20	0.13	4.57	2.43
Std	23.71	1.95	23.00	3.71	1.97	0.06	3.64	1.14

	Jammer 3							
	$\text{MVConst}_{\mathbf{e}_1}$		MVEig		MVDR		$\text{MVConst}_{\mathbf{1}}$	
	Mean	Std	Mean	Std	Mean	Std	Mean	Std
PRN01	5.68	1.48	5.13	2.05	0.04	0.04	3.95	2.09
PRN03	-5.10	1.84	-5.14	1.51	-0.13	0.04	4.87	0.49
PRN06	-37.75	2.10	-36.63	2.62	-1.54	0.07	-80.94	13.78
PRN10	53.20	1.66	51.70	4.31	-1.05	0.20	-171.76	0.60
PRN17	60.92	0.81	59.53	1.61	-2.90	0.07	-175.14	1.36
PRN23	-51.70	1.41	-50.65	1.81	2.62	0.08	2.58	0.35
PRN25	-15.74	1.39	-15.09	1.96	0.14	0.14	3.86	1.48
PRN30	6.50	1.56	6.37	2.57	-0.29	0.11	-4.82	3.09
PRN31	-0.54	2.52	-0.98	3.76	0.38	0.19	168.01	8.59
RMS	34.94	1.70	34.07	2.63	1.45	0.12	102.76	5.60
Std	34.90	0.46	34.03	0.92	1.42	0.06	98.95	4.34

be used for PPP, if an incoming jammer has a low elevation and all used satellites have a higher elevation. For other cases additional research is necessary.

REFERENCES

[1] M. Cuntz, A. Konovaltsev, M. Sgammini, C. Hattich, G. Kappen, M. Meurer, A. Hornbostel, and A. Dreher, "Field test: Jamming the DLR adaptive antenna receiver," in *ION GNSS+ 2011), Portland, OR, USA*, vol. 2023, 2011, p. 384 392.

[2] M. Meurer, A. Konovaltsev, M. Appel, and M. Cuntz, "Direction-of-Arrival Assisted Sequential Spoofing Detection and Mitigation," in *ION ITM 2016*, 2016, p. 12.

[3] E. Tasdemir, "Blind Interference Mitigation in Multi-Antenna GNSS Receivers," Dissertation, RWTH Aachen University, Aachen, Jul. 2018.

[4] Q. Jia, R. Wu, W. Wang, D. Lu, and L. Wang, "Adaptive blind anti-jamming algorithm using acquisition information to reduce the carrier phase bias," *GPS Solutions*, vol. 22, no. 4, p. 99, Jul. 19, 2018.

[5] S. Daneshmand, T. Marathe, and G. Lachapelle, "Millimetre Level Accuracy GNSS Positioning with the Blind Adaptive Beamforming Method in Interference Environments," *Sensors (Basel, Switzerland)*, vol. 16, no. 11, Oct. 31, 2016.

[6] T. Bamberg and M. Meurer, "Characterizing the carrier phase distortions for different interference mitigation approaches using an antenna array," in *ION GNSS+ 2019*, Miami, Florida, Oct. 11, 2019, pp. 3517–3527.

[7] S. Zorn, M. Niestroj, S. Caizzone, M. Brachvogel, and M. Meurer, "Self-contained Antenna Crosstalk and Phase Offset Calibration by Jointly Solving the Attitude Estimation and Calibration Problem," in *ION GNSS+ 2017*, Portland, Orgeon, USA, Jul. 7, 2017.

[8] S. Zorn, T. Bamberg, and M. Meurer, "Accurate Position and Attitude Determination in a Jammed or Spoofed Environment Using an Uncalibrated Multi-Antenna-System," in *ION ITM 2018*, 2018, p. 13.

[9] H. Xu, X. Cui, and M. Lu, "Effects of power inversion spatial only adaptive array on GNSS receiver measurements," *Tsinghua Science and Technology*, vol. 23, no. 2, pp. 172–183, Apr. 2018.

[10] M. Sgammini, F. Antreich, L. Kurz, M. Meurer, and T. G. Noll, "Blind Adaptive Beamformer Based on Orthogonal Projections for GNSS," in *ION GNSS+ 2012*, p. 10.

[11] M. V. T. Heckler, M. Cuntz, A. Konovaltsev, L. A. Greda, A. Dreher, and M. Meurer, "Development of Robust Safety-of-Life Navigation Receivers," *IEEE Transactions on Microwave Theory and Techniques*, vol. 59, no. 4, pp. 998–1005, Apr. 2011.